

A comparison between synthetic jets and continuous jets

B.L. Smith, G.W. Swift

Abstract Experimental measurements and flow visualization of synthetic jets and continuous jets with matched Reynolds numbers are described. Although they have the same profile shape, synthetic jets are wider and slower than matched continuous jets. The synthetic jets are examined at higher Reynolds numbers than previously studied and over a large range of dimensionless stroke lengths.

Nomenclature

b	cross-stream location where velocity is $0.5U_{cl}$
h	slot width
f	driving frequency
L_0	stroke length = $\int_0^{T/2} u_0(t) dt$
Q	volume flux
Q_0	$U_0 h$ for synthetic jet, and $Q_0 = U_{ave} h$ for continuous jet
Re_h	Reynolds number of continuous jet = $U_{ave} h / \nu$
Re_{U0}	Reynolds number of synthetic jet = $U_0 h / \nu$
t	time (with zero at start of blowing stroke)
T	driving period = $1/f$
u	measured instantaneous velocity
U	time-averaged velocity
U_{ave}	time-averaged slot velocity for continuous jet
U_{cl}	time-averaged centerline velocity
$u_0(t)$	centerline or cross-stream-averaged velocity at $x=0$ for synthetic jet
u_{max}	maximum of $u_0(t)$
U_0	$L_0 f$
x	streamwise coordinate

y cross-stream coordinate
 ν kinematic viscosity

1 Introduction

A synthetic jet is a time-averaged fluid motion generated by sufficient strong oscillatory flow at a sudden expansion. In recent years, the synthetic jet has been studied widely as a laboratory flow-control actuator. The primary advantage of the synthetic jet is that it has no net mass flux, which eliminates the need for plumbing, and, when applied to a base flow, results in unique effects not possible with steady or pulsed suction or blowing. These effects include the creation of closed recirculation and low-pressure regions (Honohan et al. 2000; Smith and Glezer 2002), and the introduction of arbitrary scales to the base flow (Smith and Glezer 1997; Honohan et al. 2000). Low-Reynolds number synthetic jets similar to the devices used in recent flow-control studies have been studied extensively, both experimentally (Smith and Glezer 1998) and numerically (Rizzetta et al. 1999; Lee and Goldstein 2000). However, if synthetic jets are to move from the laboratory to flight hardware, the Reynolds numbers must be much larger. No literature known to the authors exists on two-dimensional (2-D) synthetic jets of Reynolds numbers greater than 1,000.

Recently, the question of how synthetic jets compare to continuous jets at the same Reynolds number has received some attention. Early experiments by Smith and Glezer (1998) showed that a low Reynolds number synthetic jet has many characteristics that resemble continuous higher Reynolds number jets. A direct comparison was not made, since data on continuous jets with $Re_h = U_{ave} h / \nu < 1,000$ (where U_{ave} is the average velocity, h is the slot width, and ν is the kinematic viscosity) are scarce. More recently, low Reynolds number continuous jets were compared to a synthetic jet and pulsed jet generated from the same apparatus by Bera et al. (2001). Several aspects of the jets were examined, including jet spreading rate and velocity profiles. The results of that study are compared to the present results in Sect. 4.

The purpose of this study is to learn more about how synthetic jets resemble and differ from continuous jets and to explore the effects of some of the dimensionless parameters of synthetic jets. The experimental apparatus and measurement techniques are described in Sect. 2. The relevant length scales, velocity scales, and dimensionless parameters are discussed in Sect. 3. The results of the

Received: 9 July 2002 / Accepted: 11 November 2002
 Published online: 5 February 2003
 © Springer-Verlag 2003

B.L. Smith (✉), G.W. Swift
 Condensed Matter and Thermal Physics Group,
 Los Alamos National Laboratory, MS-K764, Los Alamos,
 NM, 87545, USA
 E-mail: bsmith@mae.usu.edu

Present address: B.L. Smith
 Utah State University, UMC 4130, Logan, UT, 84322, USA

The authors acknowledge Chris Espinoza and Ronald Haggart for their skill in the construction of the facility used in this study, and David Gardner for help with the phase-locking electronics. Comments by Frank Chambers on the original manuscript were very helpful. We acknowledge the financial support of the Los Alamos National Laboratory LDRD funds.

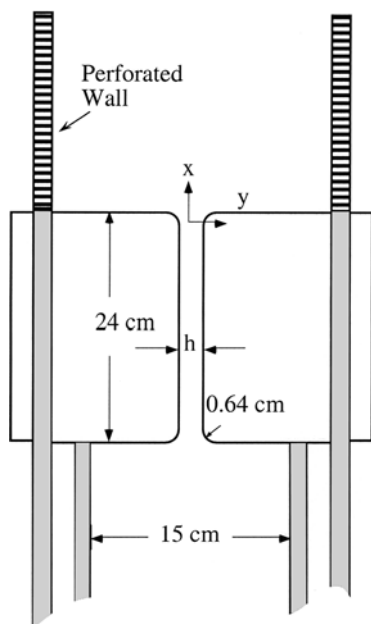


Fig. 1. Schematic of the apparatus used in this study. The nozzle blocks extend 15.2 cm into the page. Pressure oscillations are produced by a set of drivers below the nozzle. The top of the facility is open to local atmospheric pressure

comparison between the synthetic and continuous jet are presented in Sect. 4.

2 Apparatus and measurements

The experiments were performed in air at Los Alamos atmospheric pressure (78.6 kPa). The nozzle from which the jets emerge is a rectangular slot formed by two 24.1-cm long variable-position blocks (Fig. 1). The cross-stream slot width h is fixed at 0.51 cm for the experiments presented here. The spanwise length (into the page) is 15.2 cm, resulting in an aspect ratio of 30. The exit of the slot has a 0.64 cm radius to prevent flow separation during inflow. The origin of the x -axis is taken as the beginning of the exit radius rather than the exit plane (i.e., the top of the blocks), since flow visualization shows that the rollup of the vortex pairs begins there for the synthetic jets. Glass walls at the span-wise edges of the jet extend the full length of the measurement domain to help maintain a 2-D flow. The widely spaced cross-stream sidewalls downstream of the exit, which are necessary for structural reasons, are 20 cm apart and are perforated to allow relatively unimpeded air passage.

Oscillations are generated by a set of eight loudspeakers (JBL, USA), nominally rated at 600 W, attached to a plenum below the nozzle. The driver system is described in detail by Smith and Swift (2001a). The use of loudspeakers allows for a more continuous range of driving frequencies than has been achieved in the past. The facility can generate oscillating velocity amplitudes up to 50 m/s at the exit plane in the frequency range $10 < f < 100$ Hz.

A continuous jet is formed by switching off the speakers and blowing compressed air into the plenum and out the nozzle at a Reynolds number of 2,200. Hot-wire

measurements of the continuous jet indicate that the flow at the exit is laminar, symmetric, nearly fully developed, and has a fluctuation level less than 5% of the centerline mean.

Velocity measurements are made using a single straight hot wire, centered spanwise and traversed in the cross-stream and axial directions. Since the sensor is not sensitive to flow direction, measurements are limited to regions of small cross-stream velocity, such as the cross-stream centerline. The streamwise velocity profiles shown below in Fig. 5 are acquired downstream of the location where the vortex pairs cease to exist (near the peak of the time-average centerline velocity, cf. Fig. 8), and as shown by Smith and Glezer (1998), the cross-stream component of velocity is small relative to the streamwise component in this region. Systematic calibration errors are estimated to be less than 1% of the measured velocity value. The voltages from the anemometer are acquired by a 12-bit analog-to-digital converter, and each voltage sample is converted to velocity using the calibration data before averaging. Near-field measurements are made phase-locked to the driving waveform, and are phase averaged over more than 100 cycles. The velocity trace is derectified before phase averaging is performed. Profile measurements at $x=0$ are made with 100 samples per cycle, while the centerline traverses, which are used for phase-locked data near the exit plane, are performed with 40,000 samples/s regardless of the forcing frequency. Far-field profiles are sampled at 5,000 samples/s for 60 s. Even though turbulent fluctuations can be as large as 40% of the mean velocity, the large sample sizes result in a total error on mean velocity (systematic calibration error plus random error) that is dominated by the systematic error (1% of the mean flow) for every measurement. For fluctuations of 50% of the mean at a frequency that is half of the cutoff frequency (in this case, 10 kHz), the error in the mean velocity is less than 0.1% (Freythuth 1977), which is negligible in the current context. The error goes down with decreasing frequency, and the majority of the power in the flow is at frequencies much lower than 10 kHz.

Hot-wire velocity data are complemented by schlieren photographs that are taken phase-locked to the driving signal. A small amount (less than 2% of volume flow based on U_0 or U_{ave}) of hydrofluorocarbon R134a (density roughly 4 times that of air) is introduced below the nozzle blocks before the image is acquired to create the necessary gradients in the index of refraction. Confirmation that the phase-locked position and size of the vortex pairs are not affected by the flow rate of the R134a was made visually by cutting the flow by 50% and then by 75%. In all three cases, the vortex pair size and position were found to be the same.

3 Scales and dimensionless parameters

In order to facilitate a comparison between a synthetic jet and a continuous jet, we need to choose a velocity scale for the synthetic jet, which has a zero mean flow rate at $x=0$. Smith and Glezer (1998) proposed the use of the velocity scale

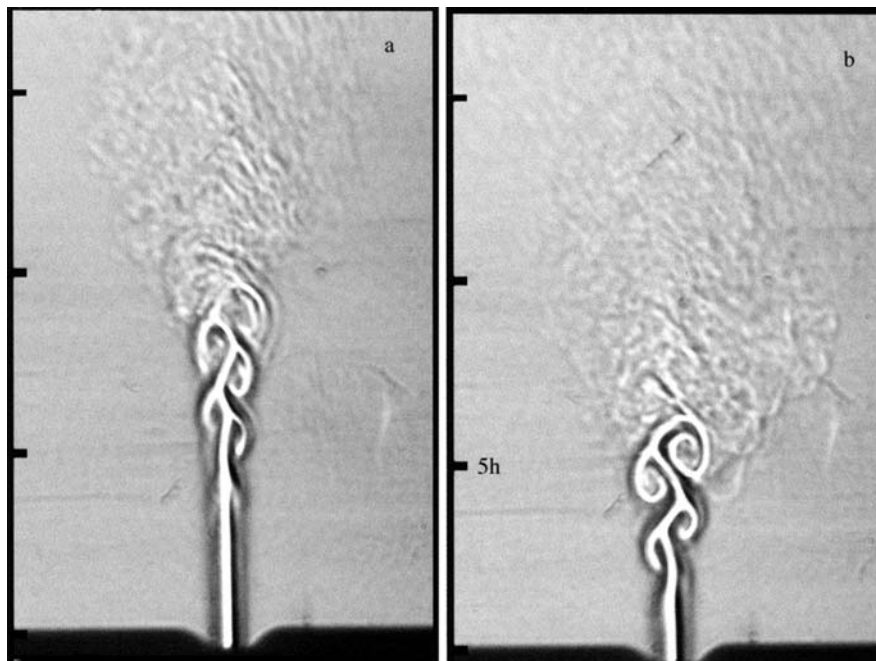


Fig. 2. Schlieren images of continuous jets with $Re_h=2,200$: a Unforced jet. b Forced jet (forcing 5.5% of mean velocity)

$$U_0 = L_0 f = \frac{1}{T} \int_0^{T/2} u_0(t) dt, \quad (1)$$

where $u_0(t)$ is the centerline slot velocity as a function of time (we will use the cross-stream average, see below), $t=0$ is the start of the blowing stroke, $T=1/f$ is the oscillation period, and L_0 (stroke length) is the length of the slug of fluid pushed from the slot during the blowing stroke. (In general, time-averaged velocities are capitalized in this paper.) Other workers have used the maximum velocity u_{\max} (which is π times U_0 for purely sinusoidal oscillations) or the rms velocity at the exit plane as the velocity scale. Note that U_0 is neither the time average of u_0 over a cycle T nor its time average over a time $T/2$. Instead, U_0 is essentially the downstream-directed velocity, which occurs only during the blowing half of the cycle, averaged over the full cycle. Smith and Glezer argued for use of U_0 in comparison with U_{ave} in a continuous jet because they believed that the average of *downstream-directed* volume flux controls the important jet phenomena.

For this nozzle, the outward flow resembles oscillatory pipe flow (Ohmi et al. 1982), while the inward flow is much more slug-like. For the synthetic jets, the Reynolds number is defined as $Re_{U_0} = U_0 h / \nu$. For the continuous jets, the cross-stream averaged velocity U_{ave} is used as the velocity scale, and the Reynolds number is defined as $Re_h = U_{\text{ave}} h / \nu$. Continuous and synthetic jets with matched Reynolds numbers based on these definitions will be referred to as “matched” herein.

The maximum entrance length over which an oscillatory flow can develop is L_0 since the flow reverses after traversing this distance. For synthetic jets that are created by oscillating flow exiting a channel of length $L < L_0$, the parameter L_0/L can impact the exit velocity profile and in turn the vortex pair rollup. Only the longest stroke length case reported here has $L_0 > L$, and examination of the velocity profiles for this case compared to another with the

same Reynolds number and a much smaller stroke length indicates that channel length has up to a 10% effect on the centerline velocity.

Assuming that the exit velocity profile is invariant, synthetic jets created by a sinusoidal flow are completely determined by two independent dimensionless parameters. Although many choices are possible, we will use the dimensionless stroke length L_0/h and the Reynolds number defined above.

4 Synthetic jets compared to continuous jets

In this section we will compare several features of continuous jets and synthetic jets. Six cases are studied, including two continuous jets and four synthetic jets. The jets referred to as “matched” (two of the synthetic jets and the two continuous jets) all have $Re \approx 2,000$. The two additional synthetic jets were generated such that $u_{\max} = U_{\text{ave}}$ from the two continuous jets.

A schlieren image of a continuous jet is shown in Fig. 2a. The field of view is 9.4 cm by 6.1 cm. It is clear from the image that the channel flow is laminar (as is to be expected for $Re_h=2,200$). Instability near 600 Hz results in the rollup of vortices starting at $x/h=5$, and the subsequent transition to turbulence. Since many features of continuous jets are facility dependent (e.g., virtual origin, spreading rates, etc., (Hussain and Clark 1977)), and since we are limited to a single facility, some variety in these features is introduced by forcing the continuous jet at its experimentally determined unstable frequency of 600 Hz. For the forced case, an oscillation amplitude of 5.5% of U_{ave} causes the rollup to occur closer to the exit plane (Fig. 2b) as expected (Rockwell 1972). Since the Strouhal number fh/U is the inverse of the dimensionless stroke length, it is tempting to try to make a connection between the forced continuous jet and the synthetic jets using the Strouhal number. This would be misguided, since it would

imply that a synthetic jet with $L_0/h=0.34$ has something in common with the forced continuous jet used in this study. As shown by Smith and Swift (2001b), a synthetic jet will not even form at such a small stroke length. Observation of jet-column instabilities in synthetic jets would likely require very long stroke lengths (longer than those reported in this study).

The features of the synthetic jet vary in time to a much larger extent than do those of the continuous jets. A synthetic jet ($Re_{U_0}=2,200$, $L_0/h=17.0$) is shown at $t/T=0.25$ in Fig. 3. Unlike the continuous jet, the flow exiting the nozzle is turbulent. As shown below (cf. Fig. 4), oscillatory

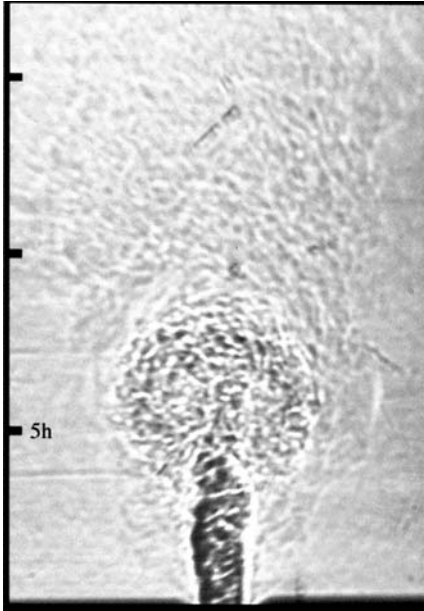


Fig. 3. Schlieren image of a synthetic jet ($L_0/h=17.0$, and $Re_{U_0}=2,200$) at $t/T=0.25$

flows with a maximum exit velocity similar to U_{ave} for the continuous jets are also turbulent over much of the blowing stroke. The remnants of the turbulent vortex pair ejected during this cycle are visible at $x/h=6$, as is the ensuing turbulent jet downstream of this point. Comparing the photographs, it is clear that cross-stream growth of the jet begins much closer to the exit plane for a synthetic jet than for a continuous jet. Based on Fig. 3, it appears that the width of the jet is similar to the size of the vortex pair in the near field.

As discussed in Sect. 3, the synthetic jet is defined by two dimensionless parameters, Re_{U_0} and L_0/h . The synthetic jet in Fig. 4a has a similar dimensionless stroke length (13.5) to the one pictured in Fig. 3, while Re_{U_0} is much lower (695). The vortex-pair structure looks comparable in size and shape to the larger Reynolds number jet shown in Fig. 3. However, careful examination (a moving picture may be required) reveals smaller-scale structure in the vortex, the stem, and the ensuing jet for the case with the higher Reynolds number. A synthetic jet with a Reynolds number nominally matched to the one in Fig. 3 but with a stroke nearly 5 times larger is shown in Fig. 4b. Since the vortex pair's position at a given time scales on L_0/h (Smith and Glezer 1998), the pair had moved out of the visualization domain long before the image was acquired. For dimensionless stroke lengths $\mathcal{O}(100)$, the vortex pair grows very rapidly and is difficult to detect in the images, perhaps because of increased mixing with the downstream fluid.

In each of these cases the vortex pair appears to be turbulent at all times, in contrast to the results of Smith and Glezer (1998), in which the pairs were initially laminar and consistently transitioned to turbulence when the suction stroke began. This is likely due to the flow at the $x=0$ being turbulent for much of the blowing stroke for all of the present jets. Oscillating flow can transition to turbulence at lower Reynolds numbers than steady flow

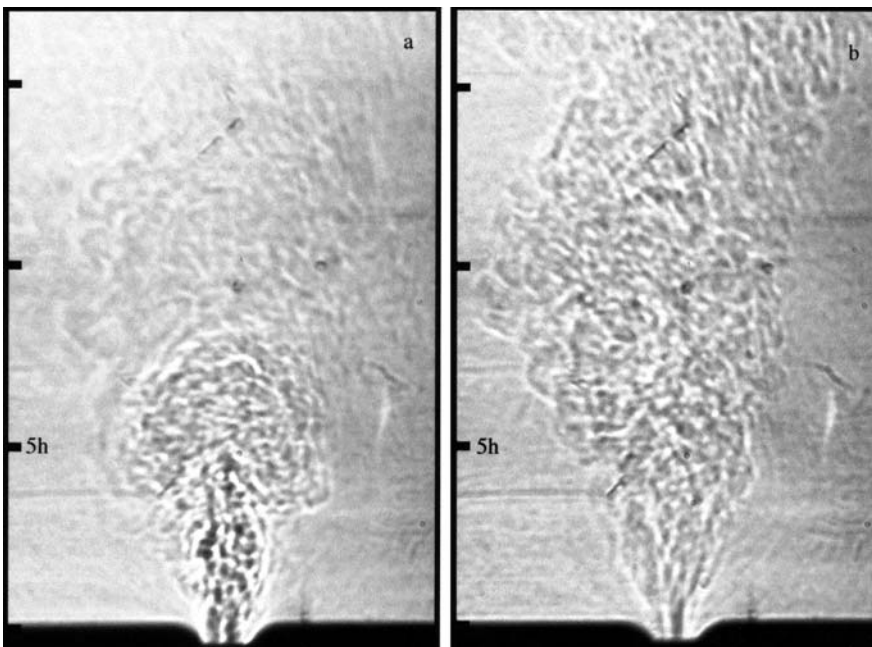


Fig. 4. Schlieren images of synthetic jets at $t/T=0.25$ with a $L_0/h=13.5$, and $Re_{U_0}=695$; and b $L_0/h=80.8$, and $Re_{U_0}=2,090$

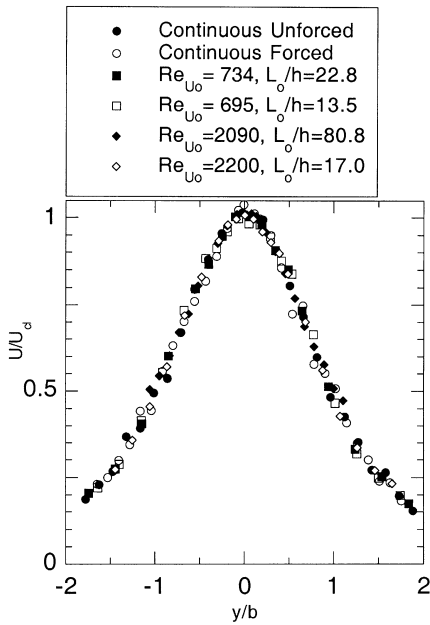


Fig. 5. Mean velocity profiles in similarity coordinates. Each profile is taken at the downstream station at which $U_{cl} \approx 0.5U_0$ or $0.5U_{ave}$

(Ohmi et al. 1982). The small Reynolds numbers used in the earlier study would likely result in laminar exiting flow. It was conjectured that the suction stroke had a destabilizing effect on the vortex pairs farther downstream.

The jets are now compared using time-averaged velocity data in the region where the jets' velocity profiles have become self-similar. Each profile was measured at the downstream station at which the centerline velocity is half of U_{ave} (continuous jets) or U_0 (synthetic jets). The velocity profiles of each jet, normalized in the usual fashion using local values of the jet width (defined below) and the maximum time-averaged velocity U_{cl} , collapse for all cases (Fig. 5). At these downstream distances, it appears that the time-averaged features of the jets exhibit little or no memory of how the jets were generated, even for the case pictured in Fig. 4b for which the profile is obtained at $x < L_0$. Profiles of synthetic jets with much smaller U_0 values also collapse to the same shape, indicating that the use of local variables for normalization renders this measurement insensitive to U_0 .

The cross-stream location at which the streamwise velocity is half of the centerline value is a commonly used quantitative measurement of the width of a jet. This jet width b is determined using the velocity profiles and is plotted in Fig. 6. The width of all of the jets grows linearly with x as is expected for 2-D continuous jets (Schlichting 1968). The data confirm that the continuous jets are narrower near the exit plane, and that the forced continuous jet is slightly wider than the unforced jet owing to increased entrainment. It also appears that the spreading rate is larger for the synthetic jets, especially for those with large stroke length. The "virtual origin," or the imaginary location where the jet width goes to zero, is generally upstream of $x=0$ for the synthetic jets, as it normally is for turbulent continuous jets. The present continuous jets are

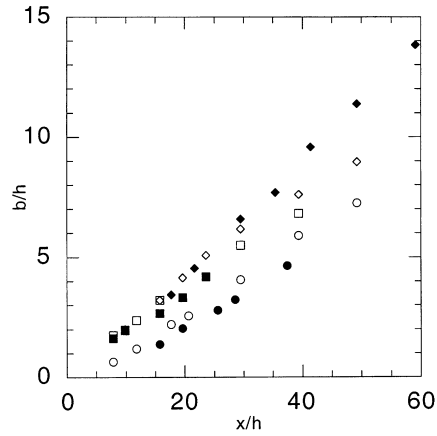


Fig. 6. Width of jet based on half maximum velocity as a function of downstream distance. Symbols as in Fig. 5

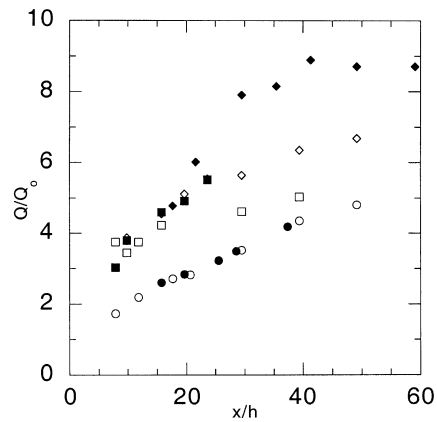


Fig. 7. Streamwise volume flux per unit depth as a function of downstream distance. Volume flux is normalized by U_0h for the synthetic jets and by $U_{ave}h$ for the continuous jets. Symbols as in Fig. 5

initially laminar and therefore do not begin linear growth until downstream of $x=0$. As a result, the virtual origin of these jets is downstream of $x=0$.

The rate at which a jet widens has a direct impact on the volume flux of the jet. Since the hot-wire measurements are limited to velocities greater than 0.5 m/s and to regions of small cross-stream velocity (compared to the local downstream velocity), the cross-stream extent of the velocity profile measurements is limited. To account for flux in the edges of the jet where measurements are not made, a theoretical (Schlichting 1968) 2-D turbulent jet profile is fitted to the data at each downstream station, and this fit is integrated to obtain the volume flux as in Smith and Glezer (1998). Specifically, it is assumed that

$$U(y) = U_{cl} \left(1 - \tanh^2 \sigma \frac{y}{x} \right), \quad (2)$$

where U_{cl} and σ are parameters of the fit. In Fig. 7, the streamwise volume flux per unit depth Q , obtained by integrating this function, is plotted for each jet versus downstream distance. The flux values are normalized by the average volume flux at the exit, $Q_0 = U_0h$ or $Q_0 = U_{ave}h$. For the two continuous jets, the flow rate increases linearly

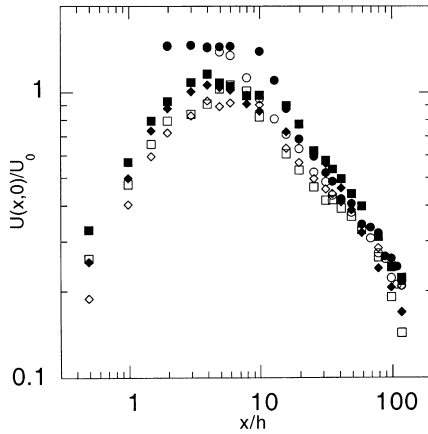


Fig. 8. Time-averaged centerline velocity versus downstream distance. Symbols as in Fig. 5

with downstream distance and is nearly identical for both cases. The synthetic jet behavior is more complicated. The synthetic jet data lie above the continuous jet values at all downstream stations because the rollup of the synthetic jet vortex pair entrains much more fluid than does the laminar continuous jet column. For the synthetic jet with $Re_{U_0}=2,200$ and $L_0/h=17$, it appears that the initial rate of increase in the volume flux with downstream distance is much larger than for the continuous jets, and that far enough downstream, dQ/dx levels off to a value closer to that of the continuous jets. For the same Reynolds number and much larger stroke length, the initial rate of increase is even larger before dropping nearly to zero at the end of the measurement domain. The growth of the volume flux of the low Reynolds number synthetic jets is also much larger for the longer stroke length case.

Similar results were reported by Bera et al. (2001). Specifically, the particle image velocimetry data from that study found that a synthetic jet ($Re_{U_0}=420$, $L_0/h=31.5$) and two continuous jets ($Re=667$ and $1,333$) had similar velocity profile shapes except for $y/b > 2$, where the synthetic jet resulted in negative velocities. In addition, Bera et al. (2001) reported that the synthetic jet was wider than the continuous jets, although by a smaller margin than shown in Fig. 6.

The fact that the forced jet is wider while its volume flux is identical to that of the unforced jet is consistent with the behavior of the centerline mean velocity shown in Fig. 8. The velocity begins to decrease from the exit value after the jet becomes turbulent (near $x/h=5$ for the forced jet; $x/h=10$ for the unforced jet). Therefore, the forcing results in a jet that is wider and slower, but of the same volume flux.

The mean velocity of synthetic jets at the exit is zero, and Fig. 8 shows that it rises to a level very near U_0 (Smith and Glezer 1998; Smith et al. 1999) (Note that the value is higher for round synthetic jets (Smith et al. 1999)) before

the $-1/2$ power-law decay typical of plane jets begins. Despite the range of Reynolds number and dimensionless stroke length in the data of Fig. 8, the centerline velocities behave essentially the same in every case. In the near field, the mean centerline velocity for the synthetic jets consistently lies below that of the continuous jets, indicating that the synthetic jets are wider and slower than matched continuous jets.

5 Conclusions

Measurements of synthetic jets with $Re_{U_0} \approx 2,000$ and $17 < L_0/h < 80$ are compared to continuous jets with the same Reynolds number. In the far field, synthetic jets bear much resemblance to continuous jets in that the self-similar velocity profiles are identical. However, in the near field, synthetic jets are dominated by vortex pairs that entrain more fluid than do continuous jet columns. Therefore, synthetic jets grow more rapidly, both in terms of jet width and volume flux, than do continuous jets.

References

- Bera JC, Michard M, Grosjean N, Comte-Bellot G (2001) Flow analysis of two-dimensional pulsed jets by particle image velocimetry. *Exp Fluids* 31:519–532
- Freythuth P (1977) Further investigation of the nonlinear theory for constant temperature hot wire anemometers. *J Phys E* 10:710–713
- Honohan AM, Amitay M, Glezer A (2000) Aerodynamic control using synthetic jets. AIAA Fluids 2000 Meeting, Denver, CO, June 2000, paper 2000-2401
- Hussain AKMF, Clark AR (1977) Upstream influence on the near field of a plane turbulent jet. *Phys Fluids* 20:1416–1425
- Lee CY, Goldstein DB (2000) Two-dimensional synthetic jet simulation. AIAA 38th Aerospace Sciences Meeting, Reno, NV, January 2000, paper 2000-0406
- Ohmi M, Iguchi M, Kakehashi K, Tetsuya M (1982) Transition to turbulence and velocity distribution in an oscillating pipe flow. *Bull JSME* 25:365–371
- Rizzetta DP, Visbal MR, Stanek MJ (1999) Numerical investigation of synthetic jet flowfields. *AIAA J* 37:919–927
- Rockwell DO (1972) External excitation of planar jets. *J Appl Mech* 39:883–890
- Schlichting H (1968) *Boundary-layer theory*. McGraw-Hill, New York
- Smith BL, Glezer A (1997) Vectoring and small-scale motions effected in free shear flows using synthetic jet actuators. AIAA 35th Aerospace Sciences Meeting, Reno, NV, 6–10 January 1997, paper 97-213
- Smith BL, Glezer A (1998) The formation and evolution of synthetic jets. *Phys Fluids* 10:2281–2297
- Smith BL, Glezer A (2002) Jet vectoring using synthetic jets. *J Fluid Mech* 458:1–34
- Smith BL, Swift GW (2001a) Measuring second-order time-averaged pressure. *J Acoust Soc Am* 110:717–723
- Smith BL, Swift GW (2001b) Synthetic jets at large Reynolds number and comparison to continuous jets. 31st AIAA Fluid Dynamics Conference, Anaheim, CA, 11–14 June 2001, paper 2001-3030
- Smith BL, Trautman MA, Glezer A (1999) Controlled interactions of adjacent synthetic jets. AIAA 37th Aerospace Sciences Meeting, Reno, NV, 11–14 January 1999, paper 99-0669